ACS central science

Research Article

http://pubs.acs.org/journal/acscii

Toward Controlled Hierarchical Heterogeneities in Giant Molecules with Precisely Arranged Nano Building Blocks

Wei Zhang,[†] Mingjun Huang,[†] Hao Su,[†] Siyu Zhang,[†] Kan Yue,[†] Xue-Hui Dong,[†] Xiaopeng Li,[‡] Hao Liu,[†] Shuo Zhang,[†] Chrys Wesdemiotis,[†,§] Bernard Lotz,[∥] Wen-Bin Zhang,*[,⊥] Yiwen Li,*[,†] and Stephen Z. D. Cheng*[,†]

[†]Department of Polymer Science, College of Polymer Science and Polymer Engineering, The University of Akron, Akron, Ohio 44325-3909, United States

[‡]Department of Chemistry and Biochemistry, Texas State University, San Marcos, Texas 78666, United States

[§]Department of Chemistry, The University of Akron, Akron, Ohio 44325-3601, United States

[∥]Institut Charles Sadron, CNRS−Université de Strasbourg, 23, Rue du Lœss, Strasbourg, 67034, France

[⊥]Key Laboratory of Polymer Chemistry & Physics of Ministry of Education, College of Chemistry and Molecular Engineering, Center for Soft Matter Science and Engineering, Peking University, Beijing 100871, China

Supporting Information

ABSTRACT: Herein we introduce a unique synthetic methodology to prepare a library of giant molecules with multiple, precisely arranged nano building blocks, and illustrate the influence of minute structural differences on their self-assembly behaviors. The T_8 polyhedral oligomeric silsesquioxane (POSS) nanoparticles are orthogonally functionalized and sequentially attached onto the end of a hydrophobic polymer chain in either linear or branched configuration. The heterogeneity of primary chemical structure in terms of composition, surface functionality, sequence, and topology can be precisely controlled and is reflected in the self-assembled supramolecular structures of these giant molecules in the condensed state. This strategy offers promising opportunities to manipulate the hierarchical heterogeneities of giant molecules via precise and modular assemblies of various nano building blocks.

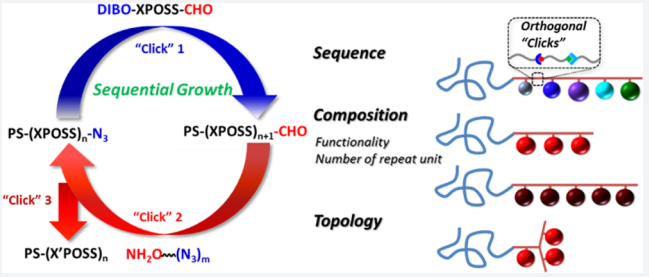

INTRODUCTION

In biological systems, the activity and function of biomacromolecules are dictated not only by their primary chemical structures but also by their secondary, tertiary, and quaternary hierarchical structures.[1−3] This is best illustrated with nuclei acids and proteins where self-assembly, molecular recognition, and replication/translation are closely associated with their functions.[3−5] In the past half-century, nature has inspired the pursuit of precision synthetic macromolecules in the field of polymer chemistry. The state-of-the-art synthetic polymers usually consist of covalently linked repeating units in various chain topologies (linear, cyclic, branched, etc.). Their properties are recognized more as a function of molecular weights, polydispersity, and chain topology, rather than the arrangement of repeating units along the chain and the collective interaction among them.[1] The precise control of sequence in polymers has been the "Holy Grail" of polymer science.[3,6−8] Many efforts have been devoted to this aspect with varying degrees of success. Recent examples include controlling the monomer sequence distribution using radical chain polymerization[9] or ring opening metathesis polymerization;[10] synthesizing sequence-defined oligomers using "click" reactions;[11−13] designing digitally encoded and information-containing macromolecule;[14] and employing DNA templates to assist efficient, sequence-specific polymerization of peptide nucleic acid aldehydes.[15,16] The classic solid state synthesis developed by Merrifield remains the gold standard for precisely defined macromolecules,[17] despite the limit at low molecular weight oligomers using small-molecule motifs.[18]

In 1960, Feynman raised a fundamental question: "*What would the properties of materials be if we could really arrange the atoms the way we want them?*".[19] In chemist's language, it is necessary not only to design and synthesize precise primary chemical structures but also to accurately control the supramolecular structures for efficiently transferring and amplifying the microscopic functions to macroscopic properties.[1,2,7,20] Echoing Feynman's question, we propose a modular approach to construct precise macromolecules using functionalized molecular nanoparticles (MNPs, or "nanoatoms") as the fundamental building blocks. It has previously been shown that T_8-POSS is an important class of model "nanoatoms".[21−24] It can be used to build up a library of POSS-based giant molecules, including giant Janus particles,[25] giant surfac-

Received: December 3, 2015
Published: January 27, 2016

DOI: 10.1021/acscentsci.5b00385
ACS Cent. Sci. 2016, 2, 48−54

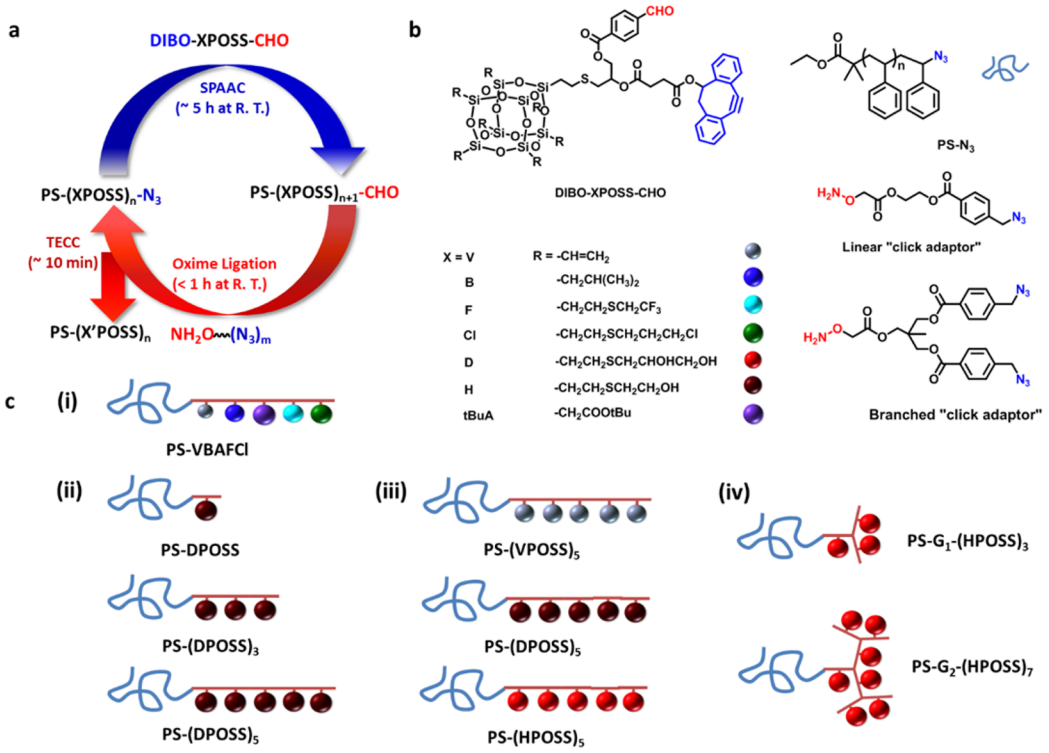

Figure 1. Synthetic routes and representative macromolecular design of giant molecules. (a) General synthetic strategy toward giant molecules. (b) The chemical structure of the POSS MNPs, PS-N_3, and the "click adaptors". (c) A library of giant molecules with controlled heterogeneities: (i) a giant molecule with distinct POSSes in a designed sequence; (ii) giant molecules with tunable number of POSSes; (iii) giant molecules with tunable functionalized POSSes; (iv) giant molecules with POSS cages arranged in dendritic topology.

tants[26,27] and giant polyhedra.[28] Other examples include giant molecules based on [60]fullerene and polyoxometalates.[29,30] Their self-assembly exhibits an unusual and remarkable sensitivity to their primary chemical structures. Hierarchically ordered supramolecular structures can be modularly built up and finely tuned in the bulk, solution, and thin films. We envision that, by attaching multiple MNPs into one giant molecule in a precisely defined sequence and geometry, their self-assembly would show controlled heterogeneity at higher length scales. A systematic study on these precise macromolecules would be critical in understanding their self-assembly and functions. In this article, we focus on the design and synthesis of giant molecules with tandem interconnected POSS cages in desirable sequences and topologies, and present a thorough evaluation of their phase structures with controlled heterogeneity.

RESULTS AND DISCUSSION

The general synthetic methodology is depicted in Figure 1a. The strategy is inspired by the solid state peptide synthesis using "click" chemistry and other highly efficient chemical transformations. Simple precipitation is used instead of the beads to improve the reaction efficiency. The use of "nanoatoms" as the fundamental building blocks greatly accelerates the modular construction of giant molecules. The basic nano building block in this case is DIBO-(XPOSS)−CHO (Figure 1b), where X represents a variety of periphery functional groups including vinyl (V), isobutyl (B), fluoroalkyl (F), and chloroalkyl (Cl), etc. The dibenzocyclooctyne (DIBO) group is ready for copper free strain-promoted azide−alkyne cycloaddition (SPAAC) and the aldehyde can undergo oxime ligation.[31,32] Those two reactions are orthogonal to each other. In addition, two kinds of small-molecule "click adaptors" (Figure 1b) are used to convert one click functionality to another without the need for protection and deprotection.[33,34] This strategy allows us to sequentially arrange the "nanoatoms" in any desired way as in Feynman's question. Notably, the architectures of resulting giant molecules can be tuned by simply using click adaptors with different geometry. In each step, purification was conveniently achieved by repeated precipitation into methanol owing to the presence of a long polystyrene tail as the purification tag. The tag can be removed if a cleavable linker is present between PS and the first POSS building block. In the present paper, we are interested in the interplay between PS chain and POSSes in self-assembly. Therefore, the linkage is kept intact. The process promises convenient and modular construction of giant molecules, which are illustrated in the following proof-of-concept examples.

For a trial to test the newly deliberated chemical synthesis route, we first designed a giant molecule with five different POSS "nanoatoms" attached along the polymeric chain in a predesigned sequence (Figure 1c.i). The entire process starts from azido-terminated polymer (i.e., PS_{135}-N_3, Figure 1b). The first SPAAC reaction installs the first XPOSS onto the polymer tail, affording the macromolecular precursor with an aldehyde chain end. The complete reaction is confirmed by the disappearance of the characteristic vibrational band of the azido group in Fourier transform infrared spectroscopy (FT-IR) at 2100 cm^{-1} (Figure S6) and appearance of an aldehyde peak at δ 10 ppm in the ^{1}H NMR (Figure S2). A "click" adaptor is used to reinstall the azido functionality, as shown by the disappearance of the chemical shift signal of aldehyde in ^{1}H NMR (Figure S3).[33,35] The cycle is then repeated. Only a slight excess of reactants relative to that of the polymer (typically

DOI: 10.1021/acscentsci.5b00385
ACS Cent. Sci. 2016, 2, 48−54

1.05−1.2 equiv) is used to ensure a complete reaction in each step instead of large excess. Near quantitative conversions were observed in a relatively short period of time under ambient conditions for each step (typically, 5 h for SPAAC and 1 h for oxime ligation).[36] After five cycles, the target molecule was obtained. The gel permeation chromatography (GPC) traces (Figure 2b) show consistent and gradual shift of the elution

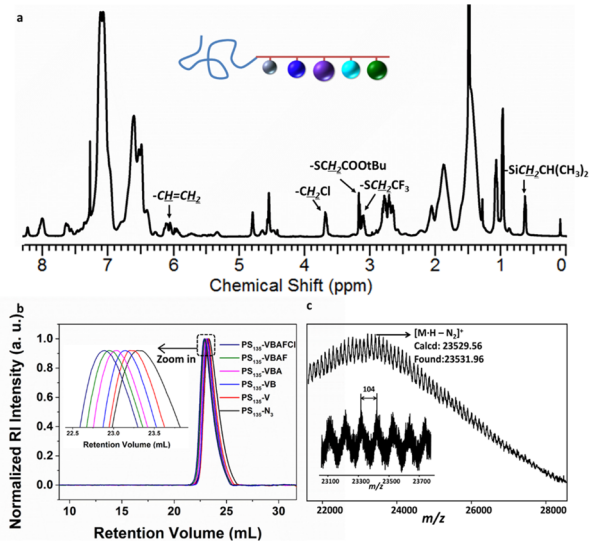

Figure 2. Characterizations of precisely synthesized giant molecules. (a) ^{1}H NMR of PS_{135}-VBAFCl, (b) GPC curves (with inserted zoomed peaks) of PS_{135}-VBAFCl and its precursors with different numbers of functionalized POSSes. (c) MALDI-TOF spectrum of PS-VBAFCl as a proof of concept. (The inset figure is zoomed in. The distance between each peak is 104, which corresponds to the molecular weight of one styrene unit.)

profile toward lower retention volumes as more POSSes are added (PDI < 1.1). The complex composition of these distinct nanoparticles are visible by their representative chemical shifts in the ^{1}H NMR spectrum (Figure 2a): $-CH{=}CH_2$ (δ 6.20−5.80 ppm) on VPOSS, $-SiCH_2CH(CH_3)_2$ (δ 0.65 ppm) on BPOSS, $-SCH_2COOtBu$ (δ 3.16 ppm) on tBuAPOSS, $-SCH_2CF_3$ (δ 3.10 ppm) on FPOSS, and $-CH_2Cl$ (δ 3.68 ppm) on ClPOSS. The successful synthesis was also confirmed by the MALDI-TOF mass spectrum (Figure 2c). In total 10 steps of reaction, the MW of the product increases progressively up to ∼24000 Da. The yields are more than 90% in each step, demonstrating the robustness of the synthetic strategy. No long-range ordered self-assembly structure was observed in this complicated giant molecule PS135-VBAFCl since both the PS and POSS domains composed of diverse VBAFCl POSS cages are hydrophobic with relatively small Flory−Huggins interaction parameters. We then proceeded to synthesize a variety of giant molecules with designed heterogeneities, including varied composition, functionality, and topology, for a systematic screening of their self-assembly behaviors.

Generally speaking, the structure formation in giant molecules is determined jointly by the amphiphilicity/immiscibility between different parts of building blocks, compositions, numbers and sequences of the nanoparticles, and topologies.[4] The modular synthetic strategy allows us to precisely and independently control these parameters. To clearly illustrate the effect of various factors on self-assembly, the following samples were designed and prepared (see Figure 1c for cartoons). The composition effect is probed in a family of linearly configured PS_m-$(VPOSS)_n$ giant molecules with precisely defined number of POSS cages, where m represents the degree of polymerization of the PS tail (m = 27, 83, or 135) and n represents the numbers of POSSes (n = 1 to 5). The thiol−ene click coupling (TECC) reaction was then used to convert the vinyl groups into a variety of functional groups onto the POSS cages [PS_m-$(DPOSS)_n$ or PS_m-$(HPOSS)_n$] to offer the amphiphilic feature of whole molecules.[35] Similarly, the topological effect is discussed by comparison of the linear shaped giant molecules, PS_m-$(XPOSS)_n$, with their dendritic topological isomers, PS_m-Gx-$(XPOSS)_n$, where Gx represents the generation of the dendritic giant molecule (G1 or G2). Table 1 lists the representative model compounds used in this

Table 1. Summary of the Phase Structures and Dimensions of Selected Samples

sample	v_f^{POSS}	phase structure	d_1 (nm)
PS_{135}-DPOSS	0.10	BCC	12.3
PS_{83}-DPOSS	0.16	HEX	11.0
PS_{135}-$(DPOSS)_2$	0.19	HEX	15.4
PS_{135}-$(DPOSS)_3$	0.26	LAM	19.5
PS_{83}-$(DPOSS)_3$	0.36	LAM	14.3
PS_{135}-$(DPOSS)_5$	0.37	LAM	22.6
PS_{27}-DPOSS	0.37	LAM	8.08
PS_{83}-$(DPOSS)_5$	0.49	LAM	17.2
PS_{27}-$(DPOSS)_2$	0.54	DG, inverse	8.80
PS_{27}-$(DPOSS)_3$	0.63	HEX, inverse	10.0
PS_{27}-$(DPOSS)_5$	0.74	HEX, inverse	11.4
PS_{135}-$(HPOSS)_3$	0.26	HEX	16.7
PS_{135}-G1-$(HPOSS)_3$	0.26	LAM	19.5

study. A comprehensive list can be found in Table S1. In the bulk state, almost all amphiphilic giant molecules exhibit ordered supramolecular structures ranging from lamella (LAM), double gyroid (DG), hexagonal cylinder (HEX), and inversed HEX to body-centered cubic (BCC) lattices after annealing at 120 to 150 °C for several hours, as shown by small-angle X-ray scattering (SAXS) and bright field (BF) transmission electron microscopy (TEM). We show in the following discussion how the different macromolecular structures led to controlled heterogeneous hierarchical assemblies in these samples.

The effect of chemical composition of giant molecules on their self-assembled supramolecular structures can be clearly demonstrated by the linear series of PS_m-$(DPOSS)_n$ (m = 135, 83, 27, n = 1 to 5). Two parameters, the number of POSS nanoparticles (n) and the length of the polymer tail (m), determine the volume fraction of v_f^{POSS}/v_f^{PS}. When v_f^{POSS} is small (such as PS_{135}-DPOSS, v_f^{POSS} = 0.10), BCC structure (Figures 3a, 3g, and 3m) with ∼100 molecules in each sphere on average is formed, in which the PS tails of these giant molecules form the matrix and the DPOSS cages are in the spherical cores. By increasing the number of DPOSS cages or reducing the PS tail length, HEX structures of PS_{135}-$(DPOSS)_2$ and PS_{87}-DPOSS are obtained (e.g., Figures 3b, 3h, and 3n). Taking PS_{135}-$(DPOSS)_2$ as an instance, there are roughly 14 DPOSS cages closely packed in a unit volume with one DPOSS thickness (1.4 nm) along the long cylinder axis. Further increasing v_f^{POSS} to above ∼0.20, LAM structures are observed until the sample PS_{27}-$(DPOSS)_2$ with v_f^{POSS} = 0.54 exhibits the

DOI: 10.1021/acscentsci.5b00385
ACS Cent. Sci. 2016, 2, 48−54

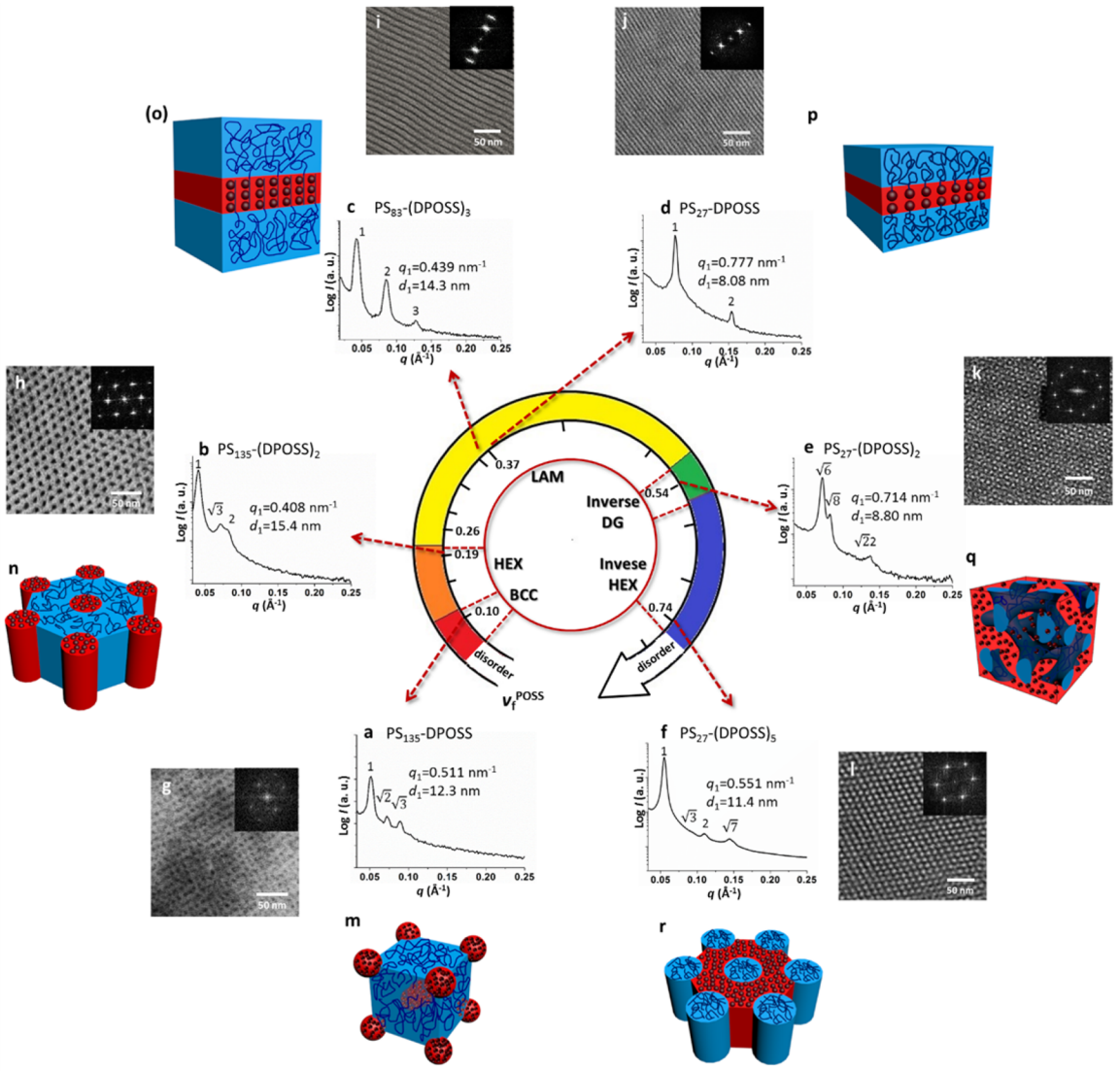

Figure 3. The effect of composition on the self-assembly behaviors of giant molecules. (a–f) Set of SAXS patterns. (g–l) Microtomed BF TEM images. (m–r) Deduced packing models of a series of selected linearly configured PS_m-$(DPOSS)_n$ samples in a phase sequence of BCC → HEX → LAM → inverse DG → inverse HEX with increasing the v_f^{POSS} value from 0.10 to 0.74. Below the v_f^{POSS} of ∼0.05 and above the v_f^{POSS} of ∼0.77, only disordered states are observed. The insets of BF TEM images are the corresponding diffraction patterns deduced from the fast Fourier transform of the images. The black bars on the v_f^{POSS} circle represent all of our samples studied.

inverse DG structure, which is confirmed by the q-ratio of $\sqrt{6}$:$\sqrt{8}$ in the SAXS pattern (Figure 3e) and the characteristic "wagon wheel" pattern along ⟨111⟩ in the BF TEM image (Figure 3k). The white regions are the PS tails embedded in the dark hydrophilic DPOSS matrix (Figure 3q). By further increasing the number of DPOSS cages in PS_{27}-$(DPOSS)_n$ (n = 3, 4, and 5), their v_f^{POSS} values reach 0.63, 0.70, and 0.74, respectively, and the inverse HEX structure is formed for these three samples. The SAXS pattern and BF TEM image (Figures 3f and 3l) are shown for PS_{27}-$(DPOSS)_5$ as an example. The PS tails are now located within the columnar cores and the partly interdigitated DPOSS cages are in the matrix (Figure 3r) with ∼12 molecules in a unit volume with one DPOSS thickness (see Supporting Information for detailed calculations).

Figure 3 illustrates the phase transitions and the corresponding SAXS patterns, BF TEM images of the linear series of PS_m-$(DPOSS)_n$ samples, and their molecular packing models at different v_f^{POSS} values. The full phase sequence can be identified as BCC → HEX → LAM → inverse DG → inverse HEX with increasing v_f^{POSS} from 0.10 to 0.74. When the v_f^{POSS} is below ∼0.05 and above ∼0.77, ordered states could not be observed. Hence, we have not yet been able to obtain the inversed BCC phases in these series of samples. Interestingly, this phase sequence is not only v_f^{POSS} dependent but also asymmetric in terms of the v_f^{POSS} due to the incommensurate shape between the DPOSS cages and the PS tails.

However, v_f^{POSS} is not the only factor that dictates the phase structure of the giant molecules. We also note that giant molecules possessing virtually the same v_f^{POSS} but different numbers of POSSes and PS tail lengths exhibit distinct self-assembly behaviors. For example, for PS_{83}-$(DPOSS)_3$ (v_f^{POSS} = 0.36), a plausible one and a half LAM packing model can be utilized to describe its assembly structure, in which the linearly configured DPOSS cages are along the layer normal, yet the head-to-head alignment is interdigitated to pack the molecules into one and a half layers as shown in Figure 3o; while in the case of PS_{27}-DPOSS (v_f^{POSS} = 0.37) with very similar v_f^{POSS}, a simple head-to-head arrangement of double layered DPOSS

DOI: 10.1021/acscentsci.5b00385
ACS Cent. Sci. 2016, 2, 48–54

and PS domains is evoked, as illustrated in Figure 3p. This is a result of the difference in cross-section ratio of DPOSS cages (~1.5 nm^2) to those of PS_{83} (~2.7 nm^2) and PS_{27} (~1.7 nm^2).[37] (See Supporting Information for detailed analysis.)

Benefiting from the modular post "click" surface functionalization of nanoparticles, various surface chemistries of POSS cages can be conveniently achieved in a modular way. A profound effect on the phase structures of these giant molecules has been observed even when their v_f^{POSS} and topology are identical. An outstanding example is PS_{135}-$(DPOSS)_3$ and PS_{135}-$(HPOSS)_3$ with an almost identical v_f^{POSS} (0.257 versus 0.260). Their phase structures are, however, HEX for PS_{135}-$(HPOSS)_3$ (Figures 4a and 4d) and LAM for PS_{135}-$(DPOSS)_3$

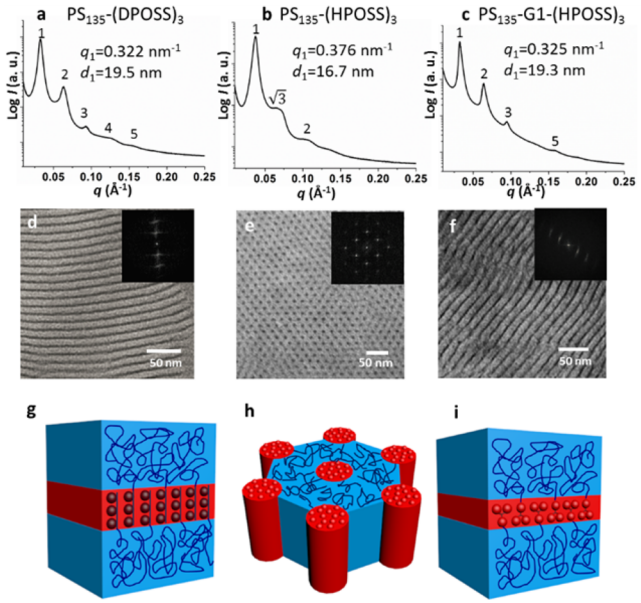

Figure 4. The effects of functionality and topology on the self-assembly behaviors of the giant molecules. (a–c) SAXS profiles. (d–f) Microtomed TEM images of PS_{135}-$(HPOSS)_3$, PS_{135}-$(DPOSS)_3$, and PS_{135}-G1-$(HPOSS)_3$, which all have v_f^{POSS} of about 0.26, to illustrate the effect of functionality and topology of POSS cages. (g–i) Cartoons illustrating the molecular packing of these structures.

(Figures 4b and 4e). Note that the significant difference almost entirely lies in the fact that each HPOSS has 7 peripheral hydroxyl groups, while each DPOSS possesses 14 hydroxyls. Since the v_f^{POSS} for PS_{135}-$(DPOSS)_3$ is slightly smaller than that for PS_{135}-$(HPOSS)_3$, the more densely packed hydroxyl groups in DPOSS cage form sturdier collective hydrogen bonds, which leads to a larger χ value and a more rigid structure in PS_{135}-$(DPOSS)_3$ compared to those in PS_{135}-$(HPOSS)_3$. It thus becomes the reason for pushing the phase across the boundary toward the LAM structure.[38,39] When more HPOSSes are attached as in PS_{135}-$(HPOSS)_4$ and PS_{135}-$(HPOSS)_5$ (Table S1), they also form LAM structures for which the one and a half layered packing scheme can be deduced as described above.

Finally, the topology of those giant molecules can be simply controlled by using small molecular "click adaptors" with the exact same reactions, which might greatly affect their supramolecular structure formation. PS_{135}-G1-$(HPOSS)_3$, with three dendritic configured HPOSS cages, and PS_{135}-$(HPOSS)_3$, with three linearly configured HPOSSes, can be considered as a pair of topological isomers. PS_{135}-$(HPOSS)_3$ has a HEX phase (Figures 4b and 4e); while the PS_{135}-G1-$(HPOSS)_3$ exhibits a LAM structure (Figures 4c and 4f). Their different structures can be again explained by incommensurateness of the cross-section areas between the HPOSS cages and the PS tails. For linearly configured PS_{135}-$(HPOSS)_3$, the cross-section areas are ~2.6 nm^2 for PS versus ~1.1 nm^2 for HPOSS (see Supporting Information), leading to a HEX structure. In PS_{135}-G1-$(HPOSS)_3$, the cross-section areas are comparable (~2.9 nm^2 for PS versus ~3.3 nm^2 for three HPOSSes, see Supporting Information), which favors the LAM structure. Interestingly, the measured layer size of the PS tails for this sample is (15.3 ± 0.4) nm, and that of HPOSS cages is about (4.0 ± 0.4) nm. We can thus deduce that the HPOSS cages in PS_{135}-G1-$(HPOSS)_3$ are head-to-head, tail-to-tail, interdigitally packed to achieve the highest packing density possible (Figure 4i).

In conclusion, we have demonstrated the design and synthesis of giant molecules with controlled hierarchical heterogeneities via different arranged nano building blocks. Taking advantage of the high selectivity and efficiency of orthogonal "click" reactions, this approach makes it possible to precisely manipulate primary structures of single macromolecules with relatively high molecular weights. It is evident that all of these hierarchical heterogeneities strongly affect the self-assembly behaviors, thereby offering a wide range of opportunities to generate rigorously controlled and fine-tuned supramolecular structures and macroscopic properties. This macromolecular engineering strategy may also be applied to a broader scope of synthetic macromolecules beyond giant molecules based on PS–POSS conjugates. Inspired by Feynman's question, we strive to create precision giant molecules with controlled heterogeneity at different length scales. Their sequence-specific, selective assembly provides a versatile platform for making precise nanostructures that are not only scientifically intriguing but also technologically relevant.

METHODS

General Procedure for SPAAC Reaction. PS_m-$(XPOSS)_n$-N_3 (1.0 equiv) and DIBO-XPOSS-CHO (1.05 equiv per $-N_3$) were added to a glass vial. THF (2 mL) was added as solvent. The mixture was stirred at ambient environment for several hours to finish, as monitored by complete disappearance of peak at 2100 cm^{-1} in FT-IR. Purification was performed by repeated precipitation into methanol to give the PS_m-$(XPOSS)_{n+1}$-CHO as white powders.

General Procedure for Oxime Ligation. PS_m-$(XPOSS)_n$-CHO (1.0 equiv) and the "click adaptor" (1.2 equiv per −CHO) were dissolved in THF (2 mL). The mixture was stirred for 2 min after triethylamine (1.2 equiv per −CHO) was added. *p*-Toluenesulfonic acid (1.2 equiv per −CHO) was then added, and the reaction mixture was stirred for about 1 h to finish, as monitored by complete disappearance of peak at 10.1 ppm in the ^1H NMR spectra. Purification was performed by repeated precipitation into methanol to give the PS_m-$(XPOSS)_n$-N_3 as white powder.

General Procedure for TECC. PS-$(VPOSS)_n$, 2 equiv of thiol ligands to vinyl group, and 0.03 equiv of photoinitiator Irgacure 2959 were dissolved in THF (2 mL). The solution was illuminated under 365 nm UV light for 10 min before precipitating into methanol/water 1:5. The products were collected by filtration.

Preparation of Bulk Samples for SAXS and Microtomed Samples for TEM. The bulk sample was placed in an aluminum holder and heated to 120 to 150 °C for 1 to 10 h

DOI: 10.1021/acscentsci.5b00385
ACS Cent. Sci. 2016, 2, 48–54

under nitrogen atmosphere. The annealed sample was directly tested in SAXS. The same sample was sliced using a microtome (LEICA EM UC7) to give thin slices with thickness <100 nm, which was transferred to carbon coated copper grids (and stained by OsO_4 overnight if necessary) for TEM experiments.

■ ASSOCIATED CONTENT

Supporting Information

The Supporting Information is available free of charge on the ACS Publications website at DOI: 10.1021/acscentsci.5b00385.

Synthetic procedures and characterization methods and data (PDF)

■ AUTHOR INFORMATION

Corresponding Authors

*S.Z.D.C.: e-mail scheng@uakron.edu.
*Y.L.: e-mail yl48@zips.uakron.edu.
*W.-B.Z: e-mail wenbin@pku.edu.cn.

Notes

The authors declare no competing financial interest.

■ ACKNOWLEDGMENTS

This work was supported by the National Science Foundation (DMR-1408872). The authors also thank Dr. Kai Guo and Zaihong Guo in Prof. Chrys Wesdemiotis's research group at the University of Akron and Prof. Zhengbiao Zhang at Soochow University for assistance with the MALDI-TOF mass spectrometry experiments.

■ REFERENCES

(1) Matyjaszewski, K. Architecturally complex polymers with controlled heterogeneity. *Science* **2011**, *333*, 1104−1105.
(2) Hawker, C. J.; Wooley, K. L. The convergence of synthetic organic and polymer chemistries. *Science* **2005**, *309*, 1200−1205.
(3) Lutz, J.-F.; Ouchi, M.; Liu, D. R.; Sawamoto, M. Sequence-controlled polymers. *Science* **2013**, *341*, 1238149.
(4) Zhang, W.-B.; Yu, X.; Wang, C.-L.; Sun, H.-J.; Hsieh, I. F.; Li, Y.; Dong, X.-H.; Yue, K.; Van Horn, R.; Cheng, S. Z. D. Molecular nanoparticles are unique elements for macromolecular science: From "Nanoatoms" to giant molecules. *Macromolecules* **2014**, *47*, 1221−1239.
(5) Zhang, W.-B.; Cheng, S. Z. D. Toward rational and modular molecular design in soft matter engineering. *Chin. J. Polym. Sci.* **2015**, *33*, 797−814.
(6) Lutz, J.-F. Polymer chemistry: A controlled sequence of events. *Nat. Chem.* **2010**, *2*, 84−85.
(7) Badi, N.; Lutz, J.-F. Sequence control in polymer synthesis. *Chem. Soc. Rev.* **2009**, *38*, 3383−3390.
(8) Li, J.; Stayshich, R. M.; Meyer, T. Y. Exploiting sequence to control the hydrolysis behavior of biodegradable PLGA copolymers. *J. Am. Chem. Soc.* **2011**, *133*, 6910−6913.
(9) Pfeifer, S.; Lutz, J.-F. A facile procedure for controlling monomer sequence distribution in radical chain polymerizations. *J. Am. Chem. Soc.* **2007**, *129*, 9542−9543.
(10) Gutekunst, W. R.; Hawker, C. J. A general approach to sequence-controlled polymers using macrocyclic ring opening metathesis polymerization. *J. Am. Chem. Soc.* **2015**, *137*, 8038−8041.
(11) Pfeifer, S.; Zarafshani, Z.; Badi, N.; Lutz, J.-F. Liquid-phase synthesis of block copolymers containing sequence-ordered segments. *J. Am. Chem. Soc.* **2009**, *131*, 9195−9197.
(12) Porel, M.; Alabi, C. A. Sequence-defined polymers via orthogonal allyl acrylamide building blocks. *J. Am. Chem. Soc.* **2014**, *136*, 13162−13165.
(13) Leibfarth, F. A.; Johnson, J. A.; Jamison, T. F. Scalable synthesis of sequence-defined, unimolecular macromolecules by Flow-IEG. *Proc. Natl. Acad. Sci. U. S. A.* **2015**, *112*, 10617−10622.
(14) Roy, R. K.; Meszynska, A.; Laure, C.; Charles, L.; Verchin, C.; Lutz, J.-F. Design and synthesis of digitally encoded polymers that can be decoded and erased. *Nat. Commun.* **2015**, *6*, 7237.
(15) Rosenbaum, D. M.; Liu, D. R. Efficient and sequence-specific DNA-templated polymerization of peptide nucleic acid aldehydes. *J. Am. Chem. Soc.* **2003**, *125*, 13924−13925.
(16) Niu, J.; Hili, R.; Liu, D. R. Enzyme-free translation of DNA into sequence-defined synthetic polymers structurally unrelated to nucleic acids. *Nat. Chem.* **2013**, *5*, 282−292.
(17) Merrifield, R. B. Solid-Phase Synthesis (Nobel Lecture). *Angew. Chem., Int. Ed. Engl.* **1985**, *24*, 799−810.
(18) Lutz, J.-F. Writing on polymer chains. *Acc. Chem. Res.* **2013**, *46*, 2696−2705.
(19) Feynman, R. P. There's plenty of room at the bottom. *Eng. Sci.* **1960**, *23*, 22−36.
(20) Mahon, C. S.; Fulton, D. A. Mimicking nature with synthetic macromolecules capable of recognition. *Nat. Chem.* **2014**, *6*, 665−672.
(21) Roll, M. F.; Asuncion, M. Z.; Kampf, J.; Laine, R. M. *para*-Octaiodophenylsilsesquioxane, $[p\text{-}IC_6H_4SiO_{1.5}]_8$, a nearly perfect nano-building block. *ACS Nano* **2008**, *2*, 320−326.
(22) Cordes, D. B.; Lickiss, P. D.; Rataboul, F. Recent developments in the chemistry of cubic Polyhedral Oligosilsesquioxanes. *Chem. Rev.* **2010**, *110*, 2081−2173.
(23) Kuo, S.-W.; Chang, F.-C. POSS related polymer nanocomposites. *Prog. Polym. Sci.* **2011**, *36*, 1649−1696.
(24) Zhang, W.; Müller, A. H. E. Architecture, self-assembly and properties of well-defined hybrid polymers based on polyhedral oligomeric silsequioxane (POSS). *Prog. Polym. Sci.* **2013**, *38*, 1121−1162.
(25) Li, Y.; Zhang, W.-B.; Hsieh, I. F.; Zhang, G.; Cao, Y.; Li, X.; Wesdemiotis, C.; Lotz, B.; Xiong, H.; Cheng, S. Z. D. Breaking symmetry toward nonspherical janus particles based on Polyhedral Oligomeric Silsesquioxanes: Molecular design, "click" synthesis, and hierarchical structure. *J. Am. Chem. Soc.* **2011**, *133*, 10712−10715.
(26) Yu, X.; Zhong, S.; Li, X.; Tu, Y.; Yang, S.; Van Horn, R. M.; Ni, C.; Pochan, D. J.; Quirk, R. P.; Wesdemiotis, C.; Zhang, W.-B.; Cheng, S. Z. D. A giant surfactant of Polystyrene−(carboxylic acid-functionalized Polyhedral Oligomeric Silsesquioxane) amphiphile with highly stretched polystyrene tails in micellar assemblies. *J. Am. Chem. Soc.* **2010**, *132*, 16741−16744.
(27) Yu, X.; Yue, K.; Hsieh, I.-F.; Li, Y.; Dong, X.-H.; Liu, C.; Xin, Y.; Wang, H.-F.; Shi, A.-C.; Newkome, G. R.; Ho, R.-M.; Chen, E.-Q.; Zhang, W.-B.; Cheng, S. Z. D. Giant surfactants provide a versatile platform for sub-10-nm nanostructure engineering. *Proc. Natl. Acad. Sci. U. S. A.* **2013**, *110*, 10078−10083.
(28) Huang, M.; Hsu, C.-H.; Wang, J.; Mei, S.; Dong, X.; Li, Y.; Li, M.; Liu, H.; Zhang, W.; Aida, T.; Zhang, W.-B.; Yue, K.; Cheng, S. Z. D. Selective assemblies of giant tetrahedra via precisely controlled positional interactions. *Science* **2015**, *348*, 424−428.
(29) Liu, H.; Hsu, C.-H.; Lin, Z.; Shan, W.; Wang, J.; Jiang, J.; Huang, M.; Lotz, B.; Yu, X.; Zhang, W.-B.; Yue, K.; Cheng, S. Z. D. Two-dimensional nanocrystals of molecular janus particles. *J. Am. Chem. Soc.* **2014**, *136*, 10691−10699.
(30) Sun, H.-J.; Tu, Y.; Wang, C.-L.; Van Horn, R. M.; Tsai, C.-C.; Graham, M. J.; Sun, B.; Lotz, B.; Zhang, W.-B.; Cheng, S. Z. D. Hierarchical structure and polymorphism of a sphere-cubic shape amphiphile based on a polyhedral oligomeric silsesquioxane−[60]-fullerene conjugate. *J. Mater. Chem.* **2011**, *21*, 14240−14247.
(31) Ning, X.; Guo, J.; Wolfert, M. A.; Boons, G.-J. Visualizing metabolically-labeled glycoconjugates of living cells by copper-free and fast Huisgen cycloadditions. *Angew. Chem., Int. Ed.* **2008**, *47*, 2253−2255.
(32) Ulrich, S.; Boturyn, D.; Marra, A.; Renaudet, O.; Dumy, P. Oxime ligation: A chemoselective click-type reaction for accessing multifunctional biomolecular constructs. *Chem. - Eur. J.* **2014**, *20*, 34−41.

DOI: 10.1021/acscentsci.5b00385
ACS Cent. Sci. 2016, 2, 48−54

(33) Su, H.; Li, Y.; Yue, K.; Wang, Z.; Lu, P.; Feng, X.; Dong, X.-H.; Zhang, S.; Cheng, S. Z. D.; Zhang, W.-B. Macromolecular structure evolution toward giant molecules of complex structure: tandem synthesis of asymmetric giant gemini surfactants. *Polym. Chem.* **2014**, *5*, 3697−3706.
(34) Yue, K.; Liu, C.; Guo, K.; Wu, K.; Dong, X.-H.; Liu, H.; Huang, M.; Wesdemiotis, C.; Cheng, S. Z. D.; Zhang, W.-B. Exploring shape amphiphiles beyond giant surfactants: molecular design and click synthesis. *Polym. Chem.* **2013**, *4*, 1056−1067.
(35) Yue, K.; Liu, C.; Guo, K.; Yu, X.; Huang, M.; Li, Y.; Wesdemiotis, C.; Cheng, S. Z. D.; Zhang, W.-B. Sequential "click" approach to Polyhedral Oligomeric Silsesquioxane-based shape amphiphiles. *Macromolecules* **2012**, *45*, 8126−8134.
(36) Tang, W.; Becker, M. L. Click" reactions: a versatile toolbox for the synthesis of peptide-conjugates. *Chem. Soc. Rev.* **2014**, *43*, 7013−7039.
(37) Chen, W. Y.; Zheng, J. X.; Cheng, S. Z. D.; Li, C. Y.; Huang, P.; Zhu, L.; Xiong, H.; Ge, Q.; Guo, Y.; Quirk, R. P.; Lotz, B.; Deng, L.; Wu, C.; Thomas, E. L. Onset of tethered chain overcrowding. *Phys. Rev. Lett.* **2004**, *93*, 028301.
(38) Dong, X.-H.; Lu, X.; Ni, B.; Chen, Z.; Yue, K.; Li, Y.; Rong, L.; Koga, T.; Hsiao, B. S.; Newkome, G. R.; Shi, A.-C.; Zhang, W.-B.; Cheng, S. Z. D. Effects of molecular geometry on the self-assembly of giant polymer−dendron conjugates in condensed state. *Soft Matter* **2014**, *10*, 3200−3208.
(39) Mammen, M.; Choi, S.-K.; Whitesides, G. M. Polyvalent interactions in biological systems: Implications for design and use of multivalent ligands and inhibitors. *Angew. Chem., Int. Ed.* **1998**, *37*, 2754−2794.

DOI: 10.1021/acscentsci.5b00385
ACS Cent. Sci. 2016, 2, 48−54